Planetary and Space Science 59 (2011) 495–501

Contents lists available at ScienceDirect

Planetary and Space Science

journal homepage: www.elsevier.com/locate/pss

Specular refection at a non-stationary shock: A simple model

K. Meziane [a,*], A.M. Hamza [a], M. Wilber [b], M.A. Lee [c], C. Mazelle [d], E.A. Lucek [e], T. Hada [f]

[a] Physics Department, University of New Brunswick, Fredericton, Canada
[b] Space Sciences Laboratory, University of California, Berkeley, United States
[c] Space Science Center, University of New Hampshire, Durham, United States
[d] Centre d'Etudes Spatiales des Rayonnements, Toulouse, France
[e] Space and Atmospheric Physics, The Blackett Laboratory, Imperial College, London, United Kingdom
[f] ESST, Kyushu University, Fukuoka, Japan

ARTICLE INFO

Article history:
Received 3 November 2009
Received in revised form
27 October 2010
Accepted 29 October 2010
Available online 21 November 2010

Keywords:
Magnetic field
Solar wind
Bow shock
Acceleration
Distribution function

ABSTRACT

Analytic treatments of a particle encountering a collisionless shock have commonly been based on the assumption that the shock surface is quasi-planar with length scales larger than the particle gyroradius. Within this framework, the particle distribution function width is supposed to be conserved in any shock reflection process. It is well known, however, that the thermal energy associated with backstreaming ions upstream of Earth's bow shock is significantly larger than the incident solar wind thermal energy. In a previous study, we found that non-thermal features of ions reflected quasi-adiabatically can be accounted for by considering the effect of small, normally distributed fluctuations of the shock normal over short temporal or spatial scales. The strong dependence of the particle acceleration on shock geometry leads to an increase in the temperature and to a non-thermal tail. Here, we conduct a similar analysis to investigate the effects of small, normally distributed fluctuations in the shock normal direction for specularly reflected ions. This later mechanism is considered of first importance in the dissipation process occurring at quasi-perpendicular shocks. We have derived the probability distribution functions $f(v_{\parallel})$ and $f(v_{\perp})$ of ions issued from a specular reflection of incident solar wind in the presence of normal direction fluctuations. These distributions deviate weakly from a Maxwellian, in agreement with the observations. In particular, a qualitative agreement with the ion thermal energy is obtained for fluctuations of the normal orientation in the 5–8° range about the nominal direction. Also, we have found that the shock θ_{Bn} has a weak effect on the shape of the distribution. While, not a strong determinant of the reflected distribution characteristics, the dynamical shock structure at ion scales cannot be ignored when accounting for the shock-accelerated particle thermal energy.

© 2010 Elsevier Ltd. All rights reserved.

1. Introduction

The ion reflection process is ubiquitous at supercritical shocks. The underlying physical processes result from a combination of magnetic and electric forces inherent within the shock layer. Two types of reflection, each with straightforward analytic solutions for post-shock encounter particle velocities, are often considered by modelers (Schwartz et al., 1983). The particle reflection is usually treated in the deHofmann–Teller frame of reference, where the convective electric field vanishes both upstream and downstream of the shock. In one case, "quasi-adiabatic reflection" occurs as a particle's incident energy and 1st adiabatic invariant is assumed to be conserved. This process satisfactorily accounts for the field-aligned beam bulk speeds observed upstream from quasi-perpendicular shocks. In a second case, "specular reflection", the normal component of the incident particle velocity is reversed while the tangential component remains unchanged. In the present report we exclusively examine the second type. (For an analysis of the first type, see Meziane et al., 2010.) As for adiabatic reflection, energy is assumed to be conserved during specular reflection. For quasi-perpendicular geometries, the guiding center velocity of a specularly reflected particle is directed downstream toward the shock (Gosling et al., 1982). Therefore, after the first encounter with the shock, following subsequent gyration upstream, the particle returns and is transmitted downstream (Gosling and Robson, 1985). These returning specularly reflected particles occupy a volume of velocity space different from the directly transmitted solar wind ions, and significantly contribute to the downstream quasi-perpendicular shock thermalization. This situation contrasts with specular reflection that occurs in quasi-parallel geometries ($\theta_{Bn} < 40^{\circ}$); in this case the particles reflect with guiding centers directed away from the shock, and easily escape upstream. Such escaping ions constitute an important source of free energy in the quasi-parallel foreshock.

* Corresponding author. Tel.: +1 506 447 3258; fax: +1 506 453 4581.
E-mail address: karim@unb.ca (K. Meziane).

0032-0633/$ - see front matter © 2010 Elsevier Ltd. All rights reserved.
doi:10.1016/j.pss.2010.10.016

Particle distributions of ions emanating from the shock and consistent with the specular reflection mechanism have been reported in previous studies, both in quasi-parallel and perpendicular foreshocks (Gosling et al., 1982; Sckopke et al., 1983; Meziane et al., 2004). Those observed in quasi-perpendicular regions are found within one gyroradius upstream from the shock ramp. Those emerging from quasi-parallel geometries are observed at various distances from the shock. To test the mechanism, significant interest was given to the velocity determination derived from the distributions' peak value. Generally, the specular reflection mechanism predicts the observed bulk speeds satisfactorily. A qualitative analysis of the specularly reflected ion distributions observed upstream of the bow shock indicates that their thermal energy is significantly larger than should be expected from reflection of the solar wind off a planar shock, which would essentially result in values comparable to that of the solar wind. The mechanism falls short in predicting the thermalization of the ion distribution.

Given that broad sections of the curved bow shock reflect ions, we might suppose that time of flight differences for fast and slow particles could be exploited to account for thermal broadening. A particle's trajectory is the result of field-aligned and convective motions, with faster particle guiding centers aligning more closely with the direction of the IMF. Consequently, fast particles arriving at a given upstream observation point will originate near where the field line threading the spacecraft contacts the shock; slow particles will have their sources further upstream. This question has been investigated more thoroughly in Meziane et al. (2010), but the important geometrical fact is that the spread of accessible source regions should increase with distance from the shock, and should therefore lead to an increase in the thermal spread. This intuitive expectation is not supported by observations within several R_E of the shock. Time of flight considerations are not of first importance in determining the shape of the velocity distributions, although we do not rule out a greater role at larger distances.

This report is an attempt to account for the thermal energy of ion distributions produced at shocks via specular reflection. It is obvious that a comprehensive understanding of these distributions is relevant since the associated population provides an important source of free energy downstream as well as upstream of the shock. Our model is motivated from studies, particularly numerical simulations, of shock non-stationarity (Hada et al., 2003; Lembège and Savoini, 1992; Scholer and Matsukiyo, 2004). A relatively recent work by Burgess (2006), based on a 2-D hybrid simulation of a supercritical quasi-perpendicular shock, showed that dynamic shock fronts accelerated electrons with greater efficiency than stationary shocks. In the present report, we employ an approach similar to that used recently for the investigation of field-aligned beam populations (Meziane et al., 2010). This later work produced model results that were satisfactory in accounting for observed features of field-aligned beams. In the next section, we briefly present some observations of specularly reflected distribution functions seen upstream of and near the shock. The mathematical model and the results are provided in Section 3. Finally, in Section 4 we discuss the model's limitations and the implications of the results, and summarize our conclusions.

2. Observations

The particle data used in the present study are from the Cluster Ion Spectrometer (CIS) experiment, which includes a Hot Ion Analyzer (HIA) and a mass spectrometer (CODIF). A detailed

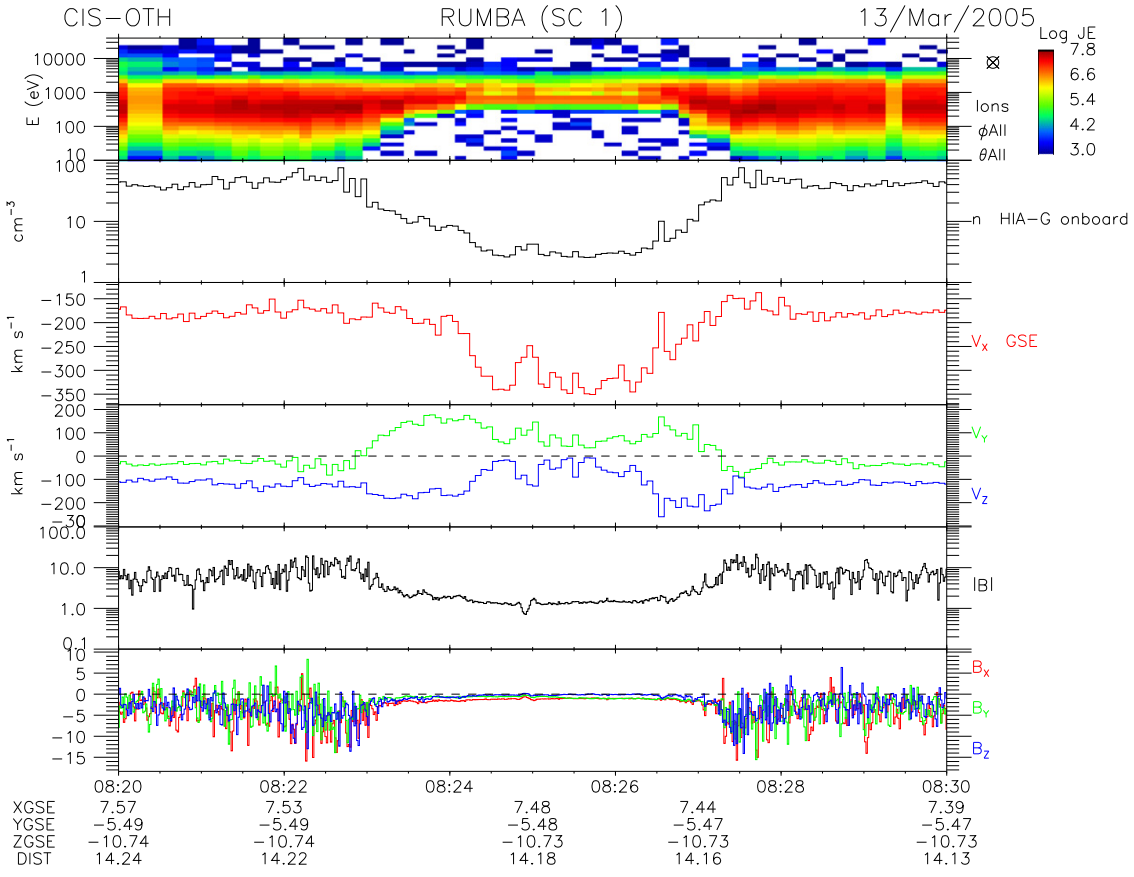

Fig. 1. Cluster SC-1 energy spectrogram (top panel), solar wind density and solar wind velocity (second to fourth panel), the magnitude (fifth panel) and the three components (bottom panel) of the magnetic field.

description of the Cluster/CIS experiment can be found in Rème (2001). We are here primarily concerned with the HIA sensor which spans energy ranges of 0.005–38 keV/q. The instrument accumulates full 3-D distributions within one 4-s satellite spin period, although during typical modes, two or three spins are averaged prior to telemetry. In burst telemetry mode, however, a HIA distribution is transmitted every spin. For the time interval presented below, the HIA sensor returned measurements from its high geometry factor side, appropriate for upstream ion measurements. Our study also uses magnetic field data, which come from the fluxgate magnetometer (Balogh et al., 2001). The spin resolution magnetic field components are used.

Fig. 1 shows particle and magnetic field data obtained by the Cluster 1 spacecraft during an inbound crossing of Earth's bow shock on 13 March 2005 between 0820 and 0830 UT. The top panel displays the energy flux spectrogram from the CIS ion experiment while the subsequent panels successively show the first two moments of the measured ion distribution, the intensity and the three components of the magnetic field. Fig. 1 clearly shows slow back and forth shock crossings due to the bow shock motions. The crossing times occur around 0823:30 and 0827:00 UT, as seen in the gradients in the ion moments and in the intensity of the magnetic field. Between the crossings the spacecraft apparently remains close to shock. While the upstream magnetic field appears quasi-steady, significant fluctuations are seen downstream; the absence of strong MHD waves indicates that the local geometry is either oblique or quasi-perpendicular. In order to determine the geometry of the shock crossings above, we have determined the shock normal using two bow shock models available in the literature (Cairns et al., 1995; Farris et al., 1991). The results obtained from both models agree well. We have found that the shock normal direction makes an angle $\theta_{Vn} \sim 150^\circ$ with the direction of the flow velocity and an angle $\theta_{Bn} \sim 71^\circ$ with the direction of the magnetic field. The value of θ_{Bn} indicates a quasi-perpendicular geometry consistent with a steady upstream magnetic field of Fig. 1. It is important to note that the particle measurements were obtained by the high geometry factor instrument (HIA-G) and therefore underestimate the plasma density (upstream and downstream); however, saturation only weakly affects the velocity moments (300–350 km s^{-1} in Fig. 1) since the solar wind beam counts continue to dominate the distributions. The narrow band below 1 keV in the energy flux spectrogram seen upstream corresponds to the solar wind ions. Although it is sometimes possible to resolve a secondary population of alpha particles at $2\times$ the energy/charge of the solar wind protons, the second band in this spectrogram has a variable energy/charge ratio, and detailed distributions (Fig. 2) show that here it includes specularly reflected ions.

We now examine a sample of ion distribution functions associated with the specularly reflected ions identified in the energy spectrogram above. Fig. 2 shows ion distributions for two snapshots taken at times where Cluster 1 is just upstream of the shock. The left columns show contour plots in the $v_\parallel - v_\perp$ system of coordinates, with the distributions sampled in the plasma rest frame of reference. The contours at zero velocity correspond to the solar wind ions, while those centered at non-zero pitch angle are

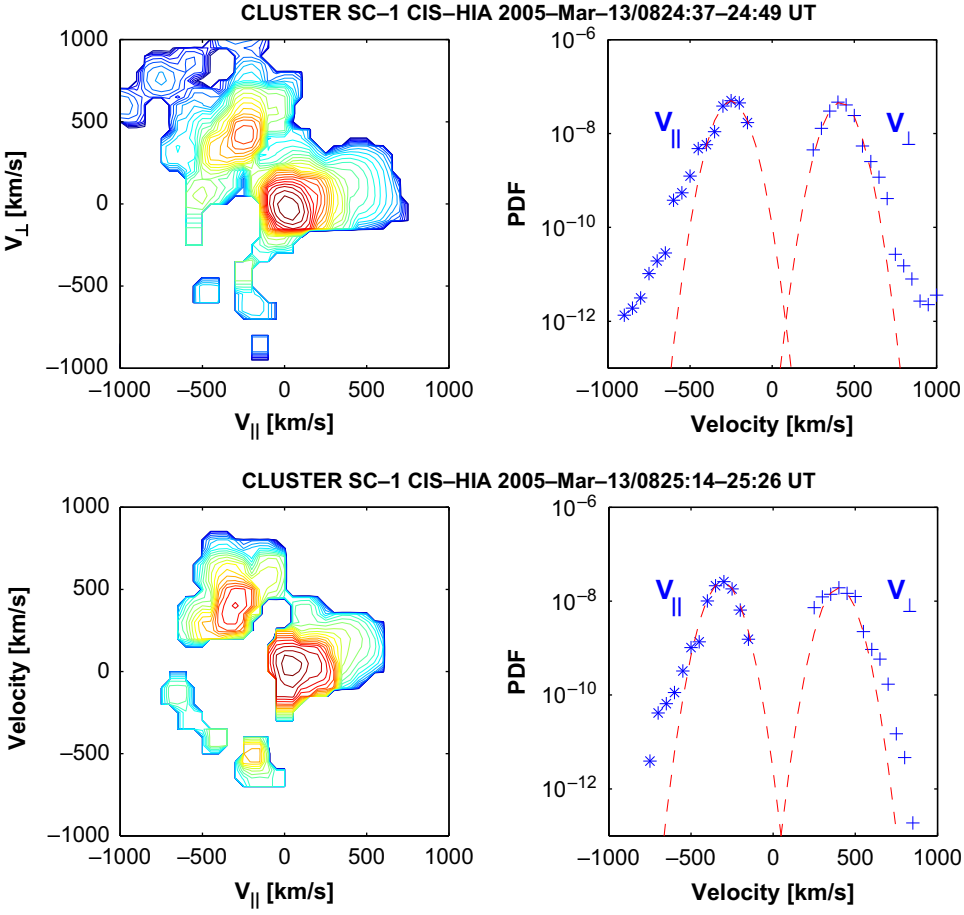

Fig. 2. The left columns show the ion velocity distribution in the $v_\parallel - v_\perp$ system of coordinates for two selected snapshots. The contours at the origin are associated with the solar wind measurement. Right columns show the reduced parallel ($V_\parallel$) and perpendicular ($V_\perp$) distribution function associated with the specularly reflected ions. A minus sign is assigned to the perpendicular velocity based on its projection along the solar wind drift velocity. The dashed red curve corresponds to the best Maxwellian fit of the data. The contour levels of the space phase density are coded such that the deep red corresponds to 10^{-6} cm^{-3}/(km s^{-1})^3 and the purple to 10^{-14} cm^{-3}/(km s^{-1})^3. (For interpretation of the references to colour in this figure legend, the reader is referred to the web version of this article.)

associated with the specularly reflected ions. The right columns show reduced perpendicular velocity distributions. In order to allow us to examine the reflected ions in isolation, we have assigned a cut-off velocity where the solar wind distribution overlaps with the specularly reflected population. The obtained reduced distributions, in which the solar wind peak has been removed, $f(v_{\parallel})$ and $f(v_{\perp})$ are fitted using a Maxwellian function $f(v) \sim \exp(-x^2/2\sigma_v^2)$, as shown by the dashed red curves. Measurements obtained in the magnetosphere's lobes show that CIS instrument has very low noise levels. Nonetheless, for our reduced distribution functions the detector background noise has been subtracted. The instrumental count rate has been estimated for each energy step and angular bin of the analyzer during time intervals when the Cluster spacecraft was outside the foreshock (in the solar wind). Background counts were obtained as closely as possible to the times of interest here. Only count rates greater than one standard deviation above the background are used. It appears that the bulk of the distribution is satisfactorily fitted by Maxwellians, although the presence of a weak tail at high energy cannot be ruled out. Therefore $\sigma_{\parallel}$ and $\sigma_{\perp}$ are good indicator of the specularly reflected population's parallel and perpendicular thermal energy. We have found that $\sigma_{\parallel} \sim \sigma_{\perp} \sim 71$ km s^{-1}, corresponding to $T=26$ eV; normalized to the solar wind speed, the thermal spread is in the range 0.21–0.24. Although saturation in CIS prevents us from using the temperature moments to characterize the solar wind beam itself, measurements from Wind and ACE upstream indicate temperatures of the order of a few eV (≤ 5 eV). While not conclusive, these and other measurements of the solar wind during quiet conditions suggest at least a factor of 3–4 increase in temperature for the specularly reflected beam.

3. Specular reflection

In this section we derive the particle distribution function of ions that are specularly reflected off a non-stationary shock. In this scenario the normal component of a particle's velocity is reversed while the transverse component remains fixed, conserving its energy, as expected in the deHoffman–Teller frame of reference. In order to explain the thermal spread, we suppose that the shock non-stationarity can be described usefully by normally distributed fluctuations in the local shock orientation about some mean, and that the beam reflection process can be taken to be instantaneous.

After transformation to the solar wind frame of reference, the normalized parallel and perpendicular velocity components of a specularly reflected ion are, respectively (Schwartz et al., 1983; Meziane et al., 2004)

$$P_{\parallel} = \frac{v_{\parallel}}{V_{sw}} = -2\cos\theta_{Vn}\cos\theta_{Bn} \tag{1}$$

$$P_{\perp} = \frac{v_{\perp}}{V_{sw}} = -2\cos\theta_{Vn}\sin\theta_{B_n} \tag{2}$$

In Eqs. (1) and (2), θ_{Bn} and θ_{V_n} are, respectively, the angles that the shock normal makes with the interplanetary magnetic field and the solar wind flow direction; θ_{Bn} is acute while θ_{Vn} is obtuse.

Ignoring small-scale surface irregularities, we could reasonably assume a locally planar shock approximation, since the large-scale shock radius of curvature is very large compared with a solar wind proton gyroradius. When both the upstream flow velocity and magnetic field direction are quasi-steady, the changes in the beam speed arise instead from variations of the local shock normal direction. Both spatial and temporal fluctuations in this may contribute to variations in the acceleration of reflected particles. Our hypothesis presupposes that upstream ions emerge from a shock that has fluctuations in the local normal orientation. The model is equally applicable to temporal variability on times scales small compared to an ion distribution sampling time as it is to spatial variability on scales small compared with the (velocity filter) accessible source region. In this perspective, the local shock normal direction $\mathbf{n}$ differs from the spatial or temporal average direction $\mathbf{n}_0$, which might be expected to agree with a normal obtained from empirical model shocks.

Let us now consider an ion that is specularly reflected off the shock where the normal direction makes an angle ϕ with respect to $\mathbf{n}_0$. To render the derivation tractable, we assume that the variations of ϕ are restricted to the BV-plane. We can write that the shock normal direction is $\mathbf{n} = (\cos\phi, \sin\phi)$ and that Eqs. (1) and (2) become

$$P_{\parallel} = -2\cos(\theta_{Vn0}-\phi)\cos(\theta_{Bn0}-\phi) \tag{3}$$

$$P_{\perp} = -2\cos(\theta_{Vn0}-\phi)\sin(\theta_{Bn0}-\phi) \tag{4}$$

where the angles θ_{Vn0} and θ_{Bn0} characterize the average local geometry based on $\mathbf{n}_0 = (1,0)$.

At this point, the nature of the variation of the shock normal direction needs to be defined. There is no physical basis for expecting that the shock normal will fluctuate randomly about its average, $\mathbf{n}_0$, although this is a reasonable and simple starting point, to be validated later. If we permit ϕ to extend to $\pm\infty$, a naive application of Eqs. (3) and (4) would include contributions for normal directions pointing into the shock. A rigorous treatment would truncate the range of ϕ such that $-\pi/2 < \theta_{Bn0}-\phi < \pi/2$, but for analytic simplicity we apply the simpler constraint $-\pi/2 < \phi < \pi/2$. As we will show below, reasonable agreement with observations can be obtained for Gaussian variations in ϕ with e-folding scales of just a few degrees. Consequently, only a small contribution in our analytic description will come from ϕ variations that reverse the shock direction. With this in mind, we write the normalized probability density function of ϕ as

$$f(\phi) = \frac{2}{\sigma_\phi\sqrt{2\pi}} \frac{\exp^{-\phi^2/2\sigma_\phi^2}}{\mathrm{erfc}\left(-\frac{\pi}{\sigma_\phi\sqrt{2}}\right) - \mathrm{erfc}\left(\frac{\pi}{\sigma_\phi\sqrt{2}}\right)} \tag{5}$$

where σ_ϕ is the standard deviation.

Given the distribution $f(\phi)$, and using Eqs. (3) and (4), it is possible to derive the distribution $f(P_{\parallel})$ and $f(P_{\perp})$ of specularly reflected ion velocities (normalized to the solar wind). Below, we carry out the derivation for $f(P_{\perp})$; $f(P_{\parallel})$ could be obtained using a similar technique. The probability that the variable $P_{\perp}$ is within the interval $[P_{\perp}\ P_{\perp}+\Delta P_{\perp}]$ is the same that the random variable ϕ is within the range $[\phi\ \phi+\Delta\phi]$; this implies

$$f(P_{\perp})\, dP_{\perp} = f(\phi)\, d\phi \tag{6}$$

which leads to

$$f(P_{\perp}) = f(\phi)\left|\frac{d\phi}{dP_{\perp}}\right| \tag{7}$$

The absolute value in the right hand side is to ensure that the probability distribution function is a positive quantity. Eq. (4) is used to calculate $d\phi/dP_{\perp}$ and the result should be expressed in term of $P_{\perp}$. This determination requires that ϕ should be expressed in term of $P_{\perp}$. For this purpose, Eq. (4) is inverted. Using some algebra, ϕ can be obtained analytically by solving the following equation:

$$\sin(\theta_{Vn0}+\theta_{Bn0})\sin^2\phi + \cos(\theta_{Vn0}+\theta_{Bn0})\sin\phi\sqrt{1-\sin^2\phi} - \left(\cos\theta_{Vn0}\sin\theta_{Bn0} - \frac{P_{\perp}}{2}\right) = 0 \tag{8}$$

We should mention that when ϕ changes the numerical value of $P_{\parallel}$ and $P_{\perp}$ always remains smaller than 2. Also, the maximum value of $P_{\perp}$ is $1+|\sin(\theta_{Vn0}-\theta_{Bn})|$.

The probability density functions $f(P_{\parallel})$ and $f(P_{\perp})$ for two numerical values of θ_{Bn} are plotted in Fig. 3; in both cases, the angle θ_{Vn0} is taken to be 160°. This choice of θ_{Vn0} is dictated by the locations where the Cluster spacecraft most frequently cross Earth's bow shock. Given that Cluster shock crossings are distant from the nose, the associated θ_{Vn} values are significantly less than 180°. A Cluster orbit survey shows that the distribution of locations of the spacecraft has a maximum at $X_{GSE} \sim 12R_E$. Using a paraboloid nominal bow shock model (Cairns et al., 1995), we have found that for this latter value of X_{GSE}, $\theta_{Vn} \sim 159°$, very close to the numerical value used in Fig. 3.

The various curves inside each panel correspond to different normal fluctuation widths σ_ϕ, as indicated. The top panels show the distributions for a quasi-parallel geometry with $\theta_{Bn0} = 40°$. The reduced parallel velocity distribution $f(P_{\perp})$ shows a velocity cut-off corresponding to the maximum specularly reflected parallel velocity given by $1-\cos(\theta_{Vn0}-\theta_{Bn0})$. The bottom panels show the distributions obtained for a quasi-perpendicular geometry ($\theta_{Bn0} = 75°$). In this case, only particles propagating away from the shock ($v_{\parallel} > 0$) are considered in $f(P_{\parallel})$. Fig. 3 shows some qualitative similarities with the observations; these include the nearly Maxwellian form of the reduced perpendicular velocity distribution function $f(P_{\perp})$. This last figure also indicates that for a fixed σ_ϕ, $f(P_{\perp})$ is wider for quasi-parallel geometries. Large variations in the fluctuations of the shock normal direction lead to higher thermal energies.

When analyzing many Cluster crossings, and based on bow shock models, we have found that overall θ_{Vn} is in the 140–165° range; it is suitable to examine the distribution profiles for various θ_{Vn} numerical values. The qualitative importance of θ_{Vn} is shown in Fig. 4 which displays the reduced distribution functions for four values of $\theta_{Vn} = 140,150$ and 170°, in the case of a quasi-parallel shock ($\theta_{Bn} = 40°$) and a quasi-perpendicular shock ($\theta_{Bn} = 75°$). The curves are plotted for a fixed value of $\sigma_\Phi = 5°$; other values of $\sigma_\Phi \leq 10°$ show similar qualitative features. Again, the velocity cut-offs seen in the distributions correspond to the maximum allowed by the specular reflection mechanism. Fig. 4 indicates that larger perpendicular thermal broadening is obtained for lower values of θ_{Vn}.

Although the specularly reflected ion distributions' cores are satisfactorily fit by Maxwellians, it is clear that the distributions appear asymmetric. In order to quantify the departure of the distributions from a Maxwellian, we have calculated their higher order moments, including the third (the skewness S) and the fourth (the kurtosis K_c). The skewness S is a measure of the extent to which particles moving in one direction (in the frame of the specularly reflected ion beam) have higher or lower speeds than those moving in the opposite direction. In plasma kinetic theory, the skewness is equivalent to the heat flux. The kurtosis K_c is a measure of how peaked the function is, with values > 0 indicating a narrow peak and a wide tail. For a Maxwellian distribution $S = 0$ and $K_c = 3$. The panels in Fig. 5 show the moments computed as a function of σ_ϕ in the 1–10° interval. Differently colored curves show the moments for a fixed numerical value of $\theta_{Vn} = 150°$, and three values of θ_{Bn0}: 40° (blue curves), 55° (green curves) and 70° (red curves). Our choice of $(\theta_{Vn},\theta_{Bn0}) = (150°,70°)$ shock is dictated by the observations of the shock presented in Fig. 1 and therefore permits a comparison with the data. We note that the bottom right panel reports the residual kurtosis $K_r = K_c - 3$. The top left panel indicates that the specularly reflected perpendicular bulk speed is nearly independent of σ_ϕ. The decrease of the mean perpendicular velocity with σ_ϕ, as it appears on Fig. 3, is compensated by the slight shift of the distribution peak towards higher velocity values. This leaves

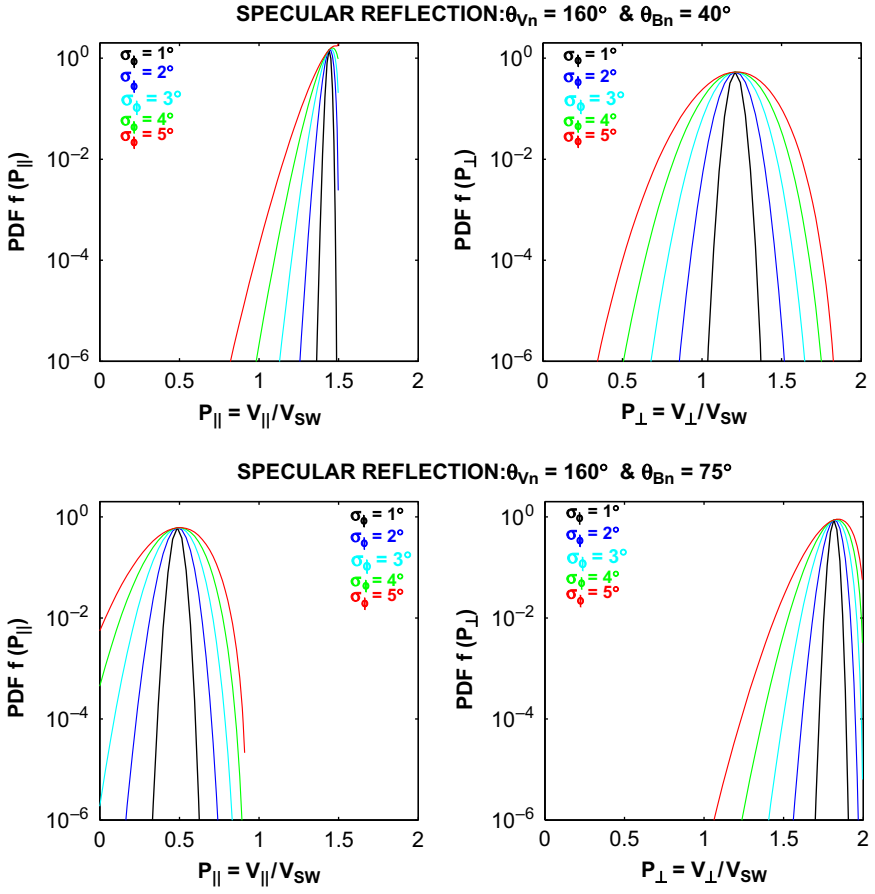

Fig. 3. Reduced parallel and perpendicular velocity distribution functions for two numerical values of $\theta_{Bn0} = 40$ and 75°; in both cases, $\theta_{Vn0} = 160°$. Both parallel and perpendicular velocities are normalized to the solar wind speed. Each curve corresponds to a value of the standard deviation σ_ϕ as indicated in the figure.

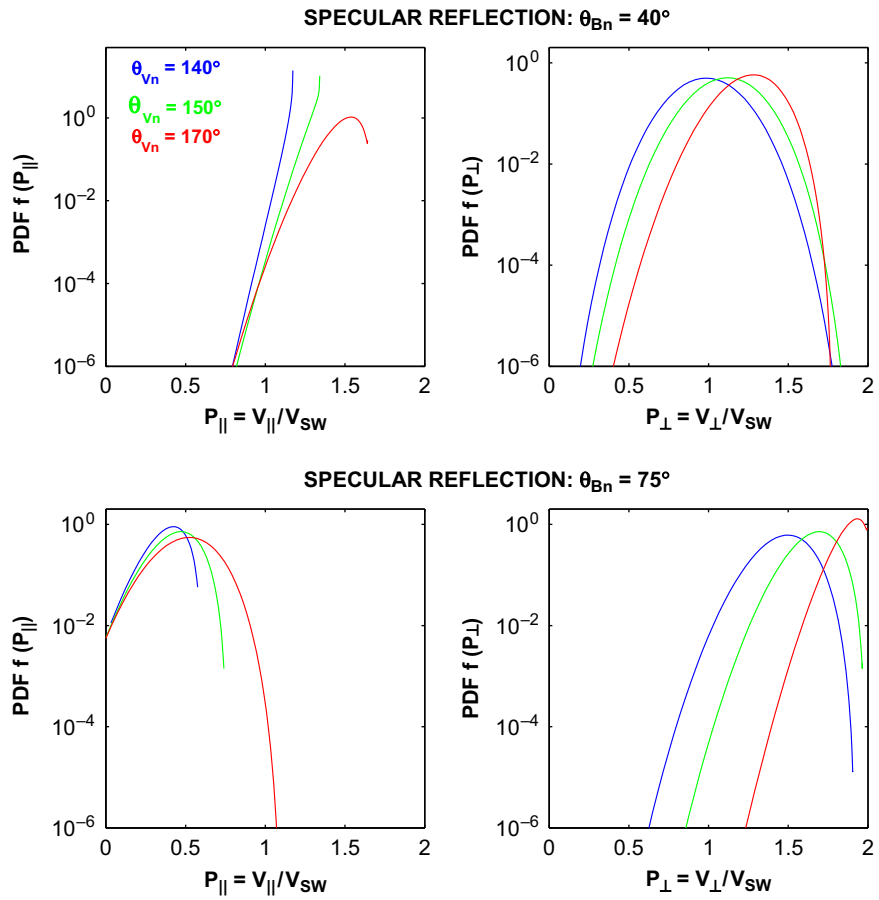

Fig. 4. Reduced parallel and perpendicular velocity distribution functions for $\theta_{Vn} = 140,150$ and 170° (blue, green and red curves, respectively) and for $\theta_{Bn0} = 40^\circ$ (top panels) and 75° (bottom panels). Both parallel and perpendicular velocities are normalized to the solar wind speed. Each curve corresponds to a fixed value of the standard deviation $\sigma_\phi = 5^\circ$. (For interpretation of the references to colour in this figure legend, the reader is referred to the web version of this article.)

the mean perpendicular velocity almost constant when σ_ϕ varies. However, there is a clear dependence upon σ_ϕ for the second (top right panel), third (bottom left panel) and fourth (bottom right panel) moments of the distribution $f(P_\perp)$. Both the first and the second moments are normalized to the solar wind speed V_{sw}. Of these higher moments, the second, $\sigma_\perp$, which can be related to the specularly reflected ions' thermal energy, has increases that are higher for quasi-parallel geometries. In particular, a quantitative agreement with the observed thermal energy is obtained for $\sigma_\phi \sim 8^\circ$. The numerical values of the skewness and the kurtosis for the reduced perpendicular distributions of Fig. 2 are $S \sim 0.30$ and $K_r \sim 0.64$, respectively; these numerical values correspond to an average obtained from the two distributions sampled in Fig. 2. A good agreement with the kurtosis is obtained in the range $\sigma_\phi \sim$ 8–10° consistent with the previous finding for $\sigma_\perp$. For the skewness, the agreement is less good since the model predicts negative skewness values.

Interestingly, the model predicts that the specular reflection produces nearly symmetric distribution functions at quasi-parallel geometries, in contrast to the quasi-perpendicular case. Similarly, the degree of flatness of $f(P_\perp)$ as measured by the kurtosis K_c seems also to increase as a second-order function of σ_ϕ.

4. Discussion

We have addressed the effects of shock normal orientation fluctuations on the specular reflection mechanism using a simple geometric model. Although the model assumes temporal changes in the shock normal direction at a specific point at the shock, the variations might also be viewed as resulting from spatial inhomogeneities at scales comparable to specularly reflected ions' gyroradii. For both views, some support is provided in the literature. Numerical simulations have shown that for moderate Mach number and low $\beta-$plasma, the quasi-perpendicular shock is nonstationary. During the reformation cycle, significant local variations arise in the shock structure. Also, a recent study using Cluster observations showed the presence of relatively small-scale oscillations in the foot and the ramp of a quasi-perpendicular bow shock (Moullard et al., 2006). It is obvious that the presence of such ripples would have a significant impact on the local shock geometry. The local shock normal fluctuations might also result from the convection of large amplitude ultra-low-frequency (ULF) waves across the shock or from solar wind turbulence, which is ubiquitous.

The 2-D geometric model used in the present work unrealistically constrains the fluctuations to a plane containing both the solar wind and the magnetic field directions (BV-plane). Although we have no basis for such restrictions, it has the advantage making the derivation tractable. Certainly a 3-D investigation is more realistic and might introduce larger fluctuation effects on the shock normal direction. As for now we restrict our results as derived from a 2-D case and the 3-D investigation will be the subject of a future study. Despite this limitation, the model satisfactorily reproduces some observed qualitative features of specularly reflected ion distribution functions. First, we have found that modeled shock normal fluctuations of $\sigma_\phi \sim 8^\circ$ agree well with the observed specularly reflected ions' thermal speeds presented above. Second, the model predicts distribution functions

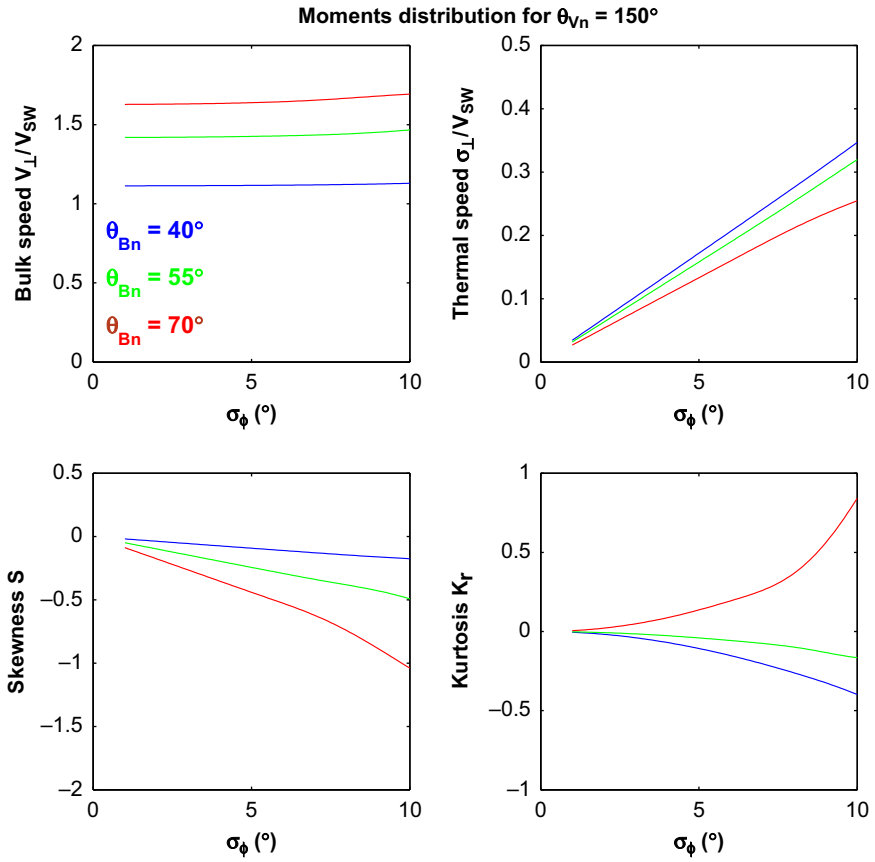

Fig. 5. First ($P_\perp = v_\perp/V_{sw}$), second ($\sigma_\perp/V_{sw}$), third (*Skewness S*) and fourth (residual *Kurtosis* K_r) order moments of the distribution $f(P_\perp)$ versus σ_ϕ for three values of θ_{Bn0}: 40° (blue curves), 55° (green curves), and 70° (red curves). (For interpretation of the references to colour in this figure legend, the reader is referred to the web version of this article.)

that are weakly skewed and weakly flattened, in agreement with the observations reported in the present work. It is important to notice that a similar analysis, applied to reflections conserving energy and the magnetic moment, and appropriate for field-aligned ion beams observed upstream of the bow shock, resulted in distribution functions that are strongly skewed (Meziane et al., 2010). Interestingly, the present model predicts features in the distribution functions that are distinct, whether the shock is quasi-parallel or perpendicular. The predicted quasi-perpendicular shock specularly reflected ion distributions have significant asymmetries and are more flattened than distributions seen at a quasi-parallel shock. A more systematic investigation of specularly reflected ion distribution functions is necessary to test the validity of the fluctuation model introduced in the present work. This will be the scope of a future study.

Acknowledgments

The authors are grateful to the International Space Science Institute for its hospitality in supporting the present work. Work at UNB has been funded by the Canadian Space Agency.

References

Balogh, A., et al., 2001. The cluster magnetic field investigation: overview of in-sight performance and initial results. Ann. Geophys. 19, 1207–1217.
Burgess, D., 2006. Simulations of electron acceleration at collisionless shocks: the effects of surface fluctuations. Astrophys. J. 653, 316–324.
Cairns, I.H., Fairfield, D.H., Anderson, R.R., Carlton, V.E.H., Paularena, K.I., Lazarus, A.J., 1995. Unusual locations of Earths bow shock on September 24–25, 1987: Mach number effects. J. Geophys. Res. 100, 47.
Farris, M.H., Petrinec, S.M., Russell, C.T., 1991. The thickness of the magnetosheath: constraints on the polytropic index. Geophys. Res. Lett. 18, 1821.
Gosling, J.T., Thomsen, M.F., Bame, S.J., Feldman, W.C., Paschmann, G., Sckopke, N., 1982. Evidence for specularly reflected ions upstream from the quasi parallel bow shock. Geophys. Res. Lett. 87, 1333–1336.
Gosling, J.T., Robson, A.E., 1985. Ion reflection, gyration, and dissipation at supercritical shocks. In: Tsurutani, B.T., Stone, G.S. (Eds.), Collisionless Shocks in the Heliosphere: Reviews of Current Research, Geophysical Monograph, vol. 35, American Geophysical Union, pp. 141–152.
Hada, T., Onishi, M., Lembège, B., Savoini, P., 2003. Shock front nonstationarity of supercritical perpendicular shocks. J. Geophys. Res. 108, 1233.
Lembège, B., Savoini, P., 1992. Nonstationarity of a two-dimensional quasi-perpendicular supercritical collisionless shock by self reformation. Phys. Fluids B 4, 3533–3548.
Meziane, K., Mazelle, C., Wilber, M., LeQuéau, D., Eastwood, J.P., Rème, H., Dandouras, I., Sauvaud, J.A., Bosqued, J.M., Parks, G.K., Kistler, L.M., McCarthy, M., Klecker, B., Korth, A., Bavassano-Cattaneo, M.-B., Lundin, R., Balogh, A., 2004. Bow shock specularly reflected ions in the presence of low frequency electromagnetic waves: a case study. J. Geophys. Res. 22, 2325–2335.
Meziane, K., Hamza, A.M., Wilber, M., Lee, M.A., Mazelle, C., Lucek, E.A., Hada, T., Markowitch, A., 2010. Effect of shock normal orientation fluctuations on field-aligned beam distributions (2010). In: Laakso, H., Taylor, M., Escoubet, C.P. (Eds.), The Cluster Active Archive, Astrophysics and Space Science Proceedings, doi 10.1007/978-90-481-3499-1-23.
Moullard, O., Burgess, D., Horbury, T.S., Lucek, E.A., 2006. Ripples observed on the surface of the quasi perpendicular bow shock. J. Geophys. Res. 111, A09113 doi: 10.1029/2005JA011594.
Rème, H., et al., 2001. First multispacecraft ion measurements in and near the Earth's magnetosphere with identical Cluster ion spectrometry (CIS) experiment. Ann. Geophys. 19, 1303–1354.
Scholer, M., Matsukiyo, S., 2004. Nonstationarity of quasi-perpendicular shocks: a comparison of full particle simulations with different ion to electron mass ratio. J. Geophys. Res. 22, 2345–2353.
Schwartz, S.J., Thomsen, M.F., Gosling, J.T., 1983. Ions upstream of the earth's bow shock: a theoretical comparison of alternative source populations. J. Geophys. Res. 88, 2039–2047.
Sckopke, N., Paschmann, G., Bame, S.J., Gosling, J.T., Russell, C.T., 1983. Evolution of ion distributions across the nearly perpendicular bow shock: specularly and non-specularly reflected gyrating ions. J. Geophys. Res. 88, 6121–6136.